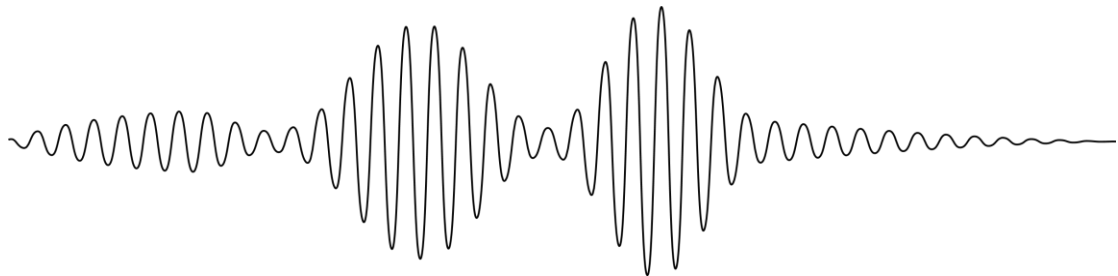




# **Hellenic Petroleum Gulf Exploration & Production of Hydrocarbons SA**



## **KYPARISSIAKOS GULF ACOUSTIC MONITORING PROJECT**

### **ITEM 1.B "Seismic noise monitoring"**

Technical Report



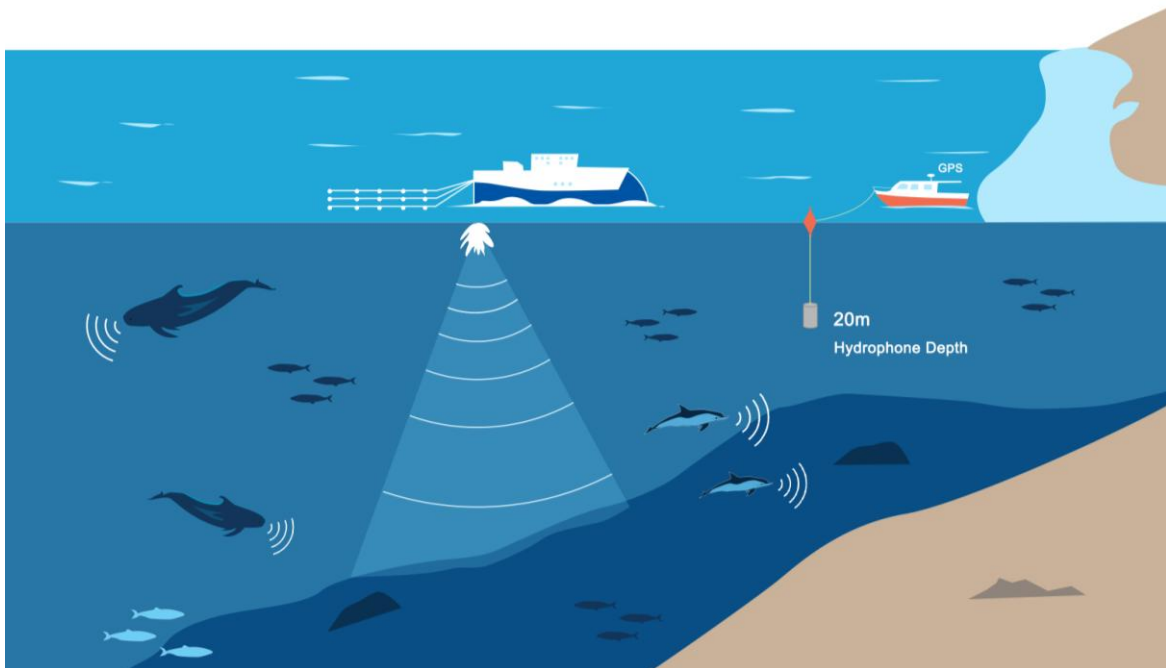
**OCEANUS LAB**

**(Laboratory of Marine Geology & Physical Oceanography)**

**Department of Geology University of Patras**

## Table of contents

1. Introduction .....	2
2. Data acquisition .....	2
3. Data Processing Methodology .....	5
3.1. Methodology overview .....	5
3.2. Airgun pulse detection and T <sub>5</sub> -T <sub>95</sub> estimation.....	6
3.3. Sound Pressure Levels .....	7
3.4. Power Spectrum Density .....	8
3.5. Approximation of relative position of “Sea Master” around SW COOK.....	8
4. Reporting material .....	9
4.1. Strofades Station .....	10
4.2. Zakynthos Station.....	11
4.3. Katakolo Station.....	12
4.4. Marathopoli Station.....	13
4.5. Methoni Station.....	14
4.6. Seismic noise VS distance to the source .....	15
5. Personnel.....	16



## 1. Introduction

The present report describes the data collection, data processing methods and the results of ITEM 1.B "Seismic noise monitoring", regarding the Kyparissiakos Gulf Acoustic Monitoring Project. The aim of the present acoustic survey was to assess the sound pressure level of the noise induced by the air-gun seismic sources to the 5 predefined sampling locations.

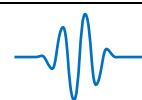
The Kyparissiakos Gulf Acoustic Monitoring Project has been planned and carried out by the Oceanus-Lab (Laboratory of Marine Geology and Physical Oceanography) of the Geology Department of the University of Patras, on behalf of the Hellenic Petroleum (HELPE).

Results presented in this report refer to acoustic data collected between January 24<sup>th</sup>, 27<sup>th</sup>, 31<sup>st</sup> and February 4<sup>th</sup>.

## 2. Data acquisition

During the seismic noise monitoring, which was carried out between January 24<sup>th</sup>, 27<sup>th</sup>, 31<sup>st</sup> and February 4<sup>th</sup>, 2022, a total of 6 deployments have been realized (table 2.1). For each station the research vessel turned off the engines to avoid any mechanical acoustic noise and deployed the underwater recording unit at 20m water depth to uninterruptedly acquire sound data for approximately two hours. In each deployment the vessel was left drifting by the winds and the sea currents, hardly stabilized by using a floating anchor. Whenever the vessel has drifted far from the intending position, correction movements were realized, the time and duration of which were noted in the logbook to be excluded from the post-survey analysis. More than 12 hours of raw data recordings have been acquired.

The navigational data of SW COOK were sent to the data processing team in a daily fashion after a valid exchange data format had been agreed. Those included time stamped coordinates of the pulse emitting Airguns from time intervals where Airgun



shots occurred. These data have been narrowed to the exact time periods where sound level recording had taken place.

Table 2.1. Seismic noise measurements sorted by date and station

Date	Strofades (S1)	Zakinthos (S2)	Katakolo (S3)	Marathopoli (S4)	Methoni (S5)
24/01/2022			√		
27/01/2022	√				
31/01/2022		√	√		
04/02/2022				√	√



Fig. 2.1. Selected pictures from the field work survey during ITEM 1.2 phase.

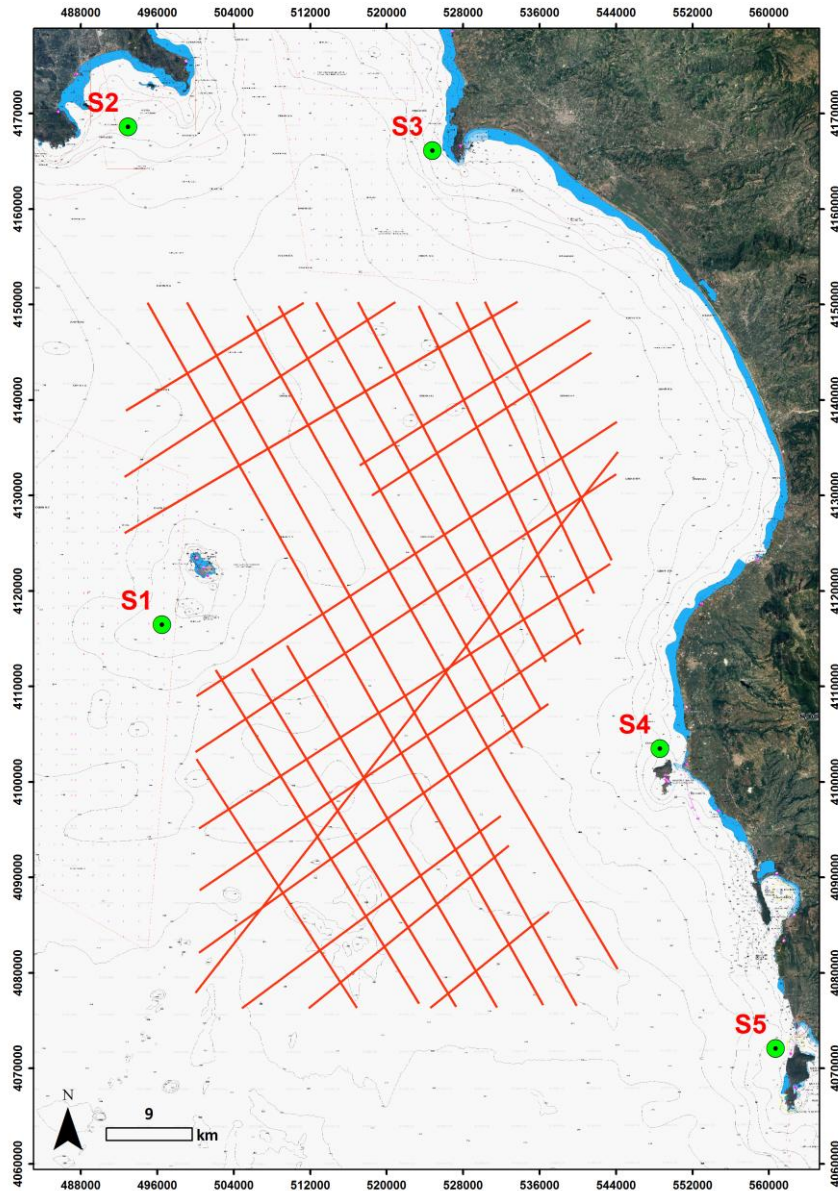


Fig. 2.2. Map locating the seismic survey area (tracklines) and the five (5) locations where spot acoustic measurements took place in the seismic monitoring phase.

### 3. Data Processing Methodology

#### 3.1. Methodology overview

The objectives of ITEM 1.B are to measure sound pressure levels induced to the predefined monitored locations by the seismic source (Airguns). To meet the above, a suite of MATLAB codes has been implemented by the Oceanus-Lab. The data processing steps were as follows:

1. Apply queries based on the operator's digital logbook entries to narrow data exclusively to effective recording times. List files by date/time and location.
2. Apply hydrophone sensitivity and digital conversion gain to digital recording units to convert to fully calibrated micropascals ( $\mu\text{Pa}$ ).
3. Apply high pass filter over 5Hz to remove the continuous components.
4. Determine start times of seismic pressure signals in digital recordings via the stored mission files by the recording unit and generate time tagged recordings.
5. Associate recording time tags to GPS fixes to georeference the recordings.
6. Calculate the instantaneous sound pressure level in dB re  $1\mu\text{Pa}$ .
7. Detect any Airgun pulses in the sound waveforms and specify time occupied by the central portion of the pulse, where 90% (T5% - T95%) of the pulse energy resides.
8. Calculate SPL<sub>p-p</sub>, SPL<sub>peak</sub>, SPL<sub>rms</sub> and SEL (as defined in the following) for every detected impulse sound (associated to air-gun pulses). All sound pressure metrics are estimated with an integration time equal to the T5% - T95% of each Airgun pulse.
9. Calculate the power spectrum density for sliding time windows of 30 seconds duration throughout the sound recordings, integrated over 1Hz (as described in paragraph 3.5.).
10. Estimate the distance and the azimuth between “Sea Master” and SW COOK for each detected impulse sound, considering their synchronized navigational



data. Use polar ( $\theta - d$ ) or Cartesian ( $x - y$ ) coordinates to estimate relative positions of SW COOK and “Sea Master”.

### 3.2. Airgun pulse detection and $T_5$ - $T_{95}$ estimation

Pulse detection and 90% pulse energy duration estimation was performed in an automatic manner first by applying a peak detector to the RMS smoothed signal and then by determining the 5% - 95% rise time of the cumulative squared signal (see fig 3.1.).

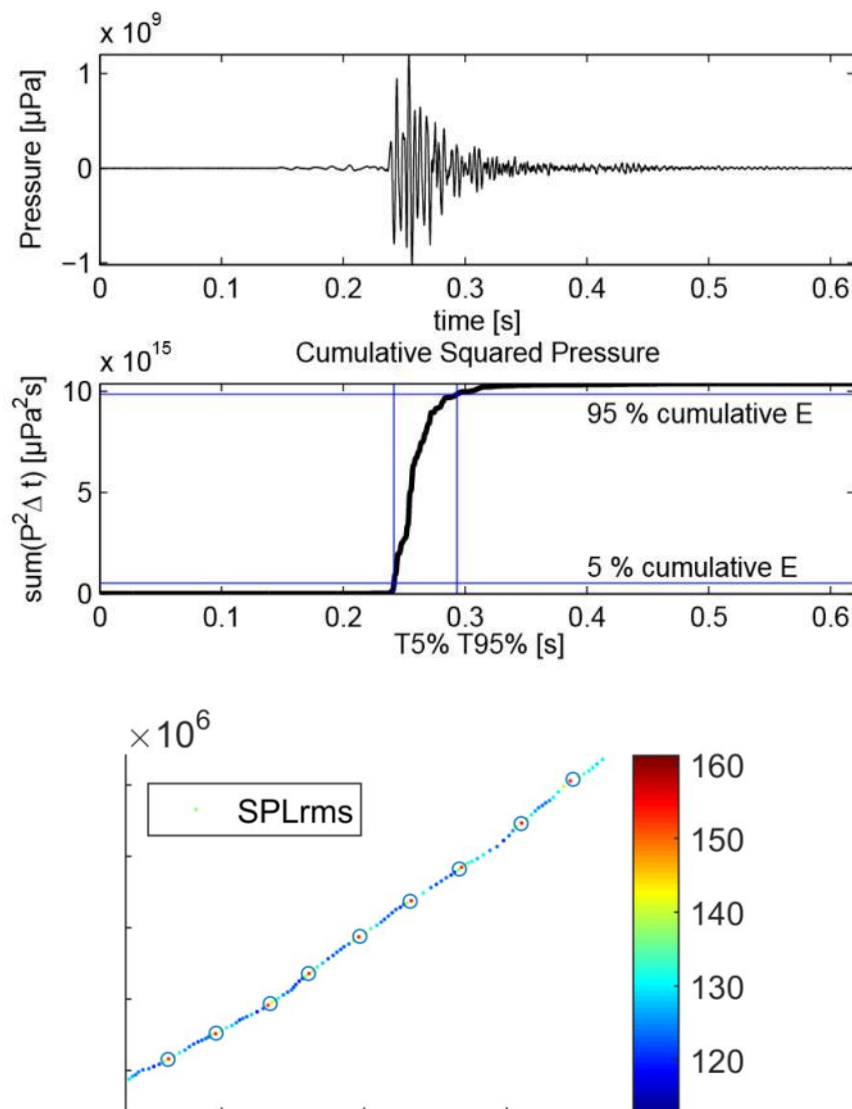


Fig. 3.1. Estimation of the 5% - 95% energy time intervals for an Airgun impulse sound through the cumulative squared pressure of the raw signal (Top Figures).

SPLrms recorded on the monitoring line (colored dots) and detected impulses (circles). Colorbar corresponds to SPLrms dB re 1  $\mu$ Pa (Bottom Figure).

### 3.3. Sound Pressure Levels

For each second of the sound recordings the SPL<sub>p-p</sub>, SPL<sub>peak</sub> and SPL<sub>rms</sub> metrics have been calculated while the SEL has additionally been calculated for each detected Airgun impulse sound (T5% - T95% integration time) using the follows formulas:

1. Peak to peak Sound Pressure Level (SPL<sub>p-p</sub>). The sum of the peak compressional pressure and the peak refractive pressure during a stated time interval. This quantity is typically most useful as a metric for a pulsed waveform.

$$SPL_{p-p} = 20 \log_{10} \frac{P_{p-p}}{1 \cdot \mu Pa}$$

where  $P_{p-p}$  is the difference between the minimum and the maximum pressure in the time interval.

2. Peak sound pressure level (SPL<sub>peak</sub>) is the maximum absolute amplitude value in the signal during a specified time interval:

$$SPL_{peak} = 20 \log_{10} \frac{P_{peak}}{1 \cdot \mu Pa}$$

where  $P_{peak}$  is the peak pressure and units are dB re 1  $\mu$ Pa.

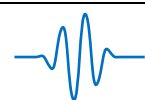
3. Root mean square (RMS) sound pressure level (SPL<sub>rms</sub>) is the log transformed square root of the average square pressure of the signal over a specific time interval:

$$SPL_{rms} = 20 \log_{10} \frac{P_{rms}}{1 \cdot \mu Pa}$$

where  $P_{rms}$  is the root mean square (rms) pressure and units are dB re 1  $\mu$ Pa.

4. Sound exposure level (SEL), is the squared sound pressure integrated over a specific duration:

$$SEL = 10 \log_{10} \left( \frac{\sum_{i=1}^n P_i^2(t)}{1 \cdot \mu Pa} \cdot \Delta t \right)$$





where P is the pressure and units are dB re 1  $\mu\text{Pa}^2\cdot\text{s}$ .

### 3.4. Power Spectrum Density

Power spectral density (PSD) is the power in the signal per unit frequency (1Hz in the present case) over the duration of the signal (30secs in the present case). The PSD was computed using Welch's method, which divides the signal into overlapping segments that are windowed. The window function was set to be a hamming one, which is optimized to decreasing the amplitude of the side-lobes in the spectrum. Frequency components have been estimated via Fast Fourier Transform (FFT). Units are dB re 1  $\mu\text{Pa}^2/\text{Hz}$ .

### 3.5. Approximation of relative position of “Sea Master” around SW COOK

In order to study the attenuation of impulse sounds around the seismic source, the relative position of “Sea Master” and each emitting Airgun of SW COOK needs to be estimated, considering SW COOK as stationary, and “Sea Master” moving around it and collecting sound level samples. A solution towards the above is to estimate the polar coordinates of “Sea Master” in relation to SW COOK at a specified time ( $t_1$ ), using the heading and x, y position of SW COOK, the distance (d) between the two vessels and the X, Y position of “Sea Master”. SW COOK's heading can be estimated using its position at two consecutive times ( $t_1$  and  $t_2$ ) while the azimuth between the two vessels ( $\theta$ ) can easily be specified using the defined triangle between “Sea Master” and the two consecutive positions of SW COOK.



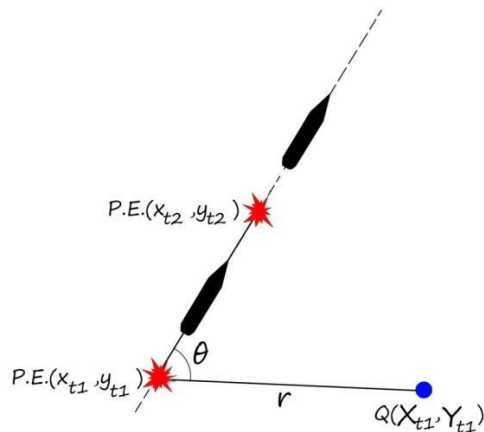


Fig. 3.2. Estimating the polar coordinates ( $\theta$ ,  $d$ ) for the relative position of Sea Master (Q) around SW Cook (P.E.) at time 1.

## 4. Reporting material

The main body of the reporting material involved the following visualizations for each station:

- a) **Spatial representation of the sound pressure levels** of the detected seismic pulses in relation to the position of the SW COOK while executing the seismic lines. SW COOK positions were delivered on a daily basis to the sound processing team and associated to the sound recordings via UTC time. Apart from the geographic coordinates, spatial representations also included a polar grid centered on the average location of the sound recordings and extended over the maximum distance between the SW COOK and the Sea Master, having radial axes with a 15 degrees angular interval.
- b) **PSD plots.** The sliding 30 seconds window integrated PSDs were combined under a single graph, using their rms value and their relative occurrence densities over 1dB intervals. The frequency axis was set to logarithmic scale to enhance low frequency components. The relative density of the PSDs (one for each 30 seconds) in the frequency versus PSD Euclidean space was presented using yellow to red color-scale, with red denoting dominant frequencies, i.e. those occurring most often in time. The lower 5% and the upper 95% quartiles have also been provided.

c) **Histogram plots.** SPL histograms offer a means of simple overview of the impact of the seismic activity in relation to the ambient noise as recorded during the ITEM 1A stage. For each station a histogram of SPLrms is provided and compared to the equivalents created from the recordings of the pre-start ambient noise monitoring, as reported in ITEM 1.A "Pre-start phase ambient noise monitoring" in Kyparissiakos Gulf.

#### 4.1. Strofades Station

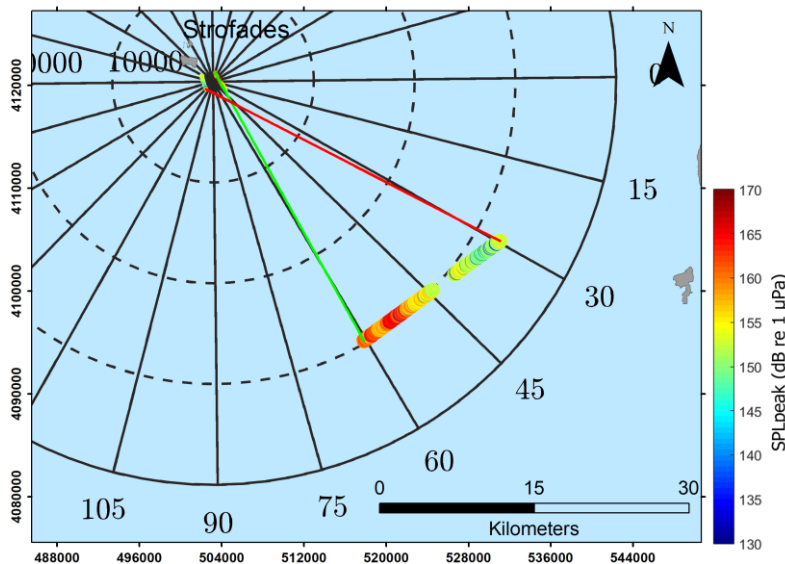


Fig. 4.1. Spatial representation of the SPLpeak of the detected seismic pulses in Strofades station, with regard to the position of the SW COOK while executing seismic lines.

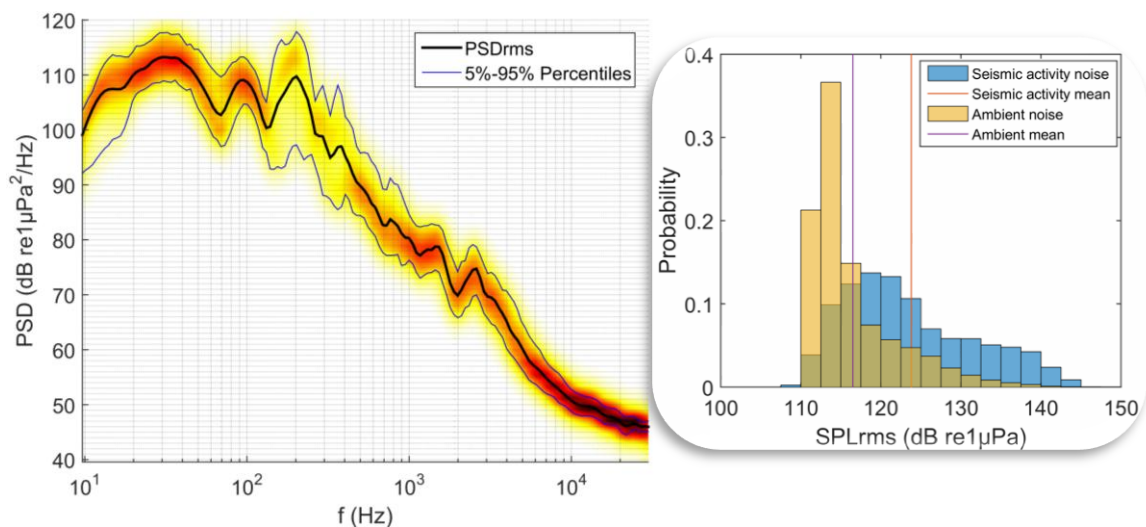


Fig. 4.2. Aggregated 30 sec PSDs concerning Strofades station and SPLrms histograms (din width 2.5 dBre1 $\mu$ Pa) with average value indications regarding seismic activity versus ambient noise monitoring.

#### 4.2. Zakynthos Station

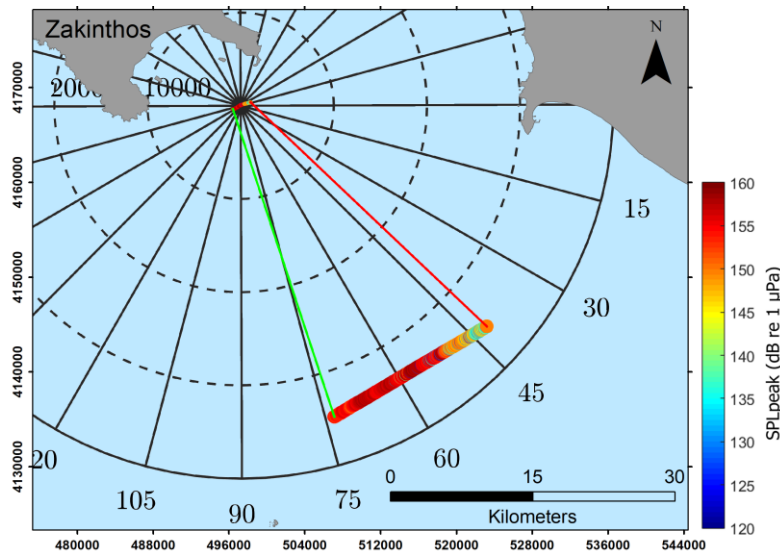


Fig. 4.3. Spatial representation of the SPLpeak of the detected seismic pulses in Zakynthos station, with regard to the position of the SW COOK while executing seismic lines.

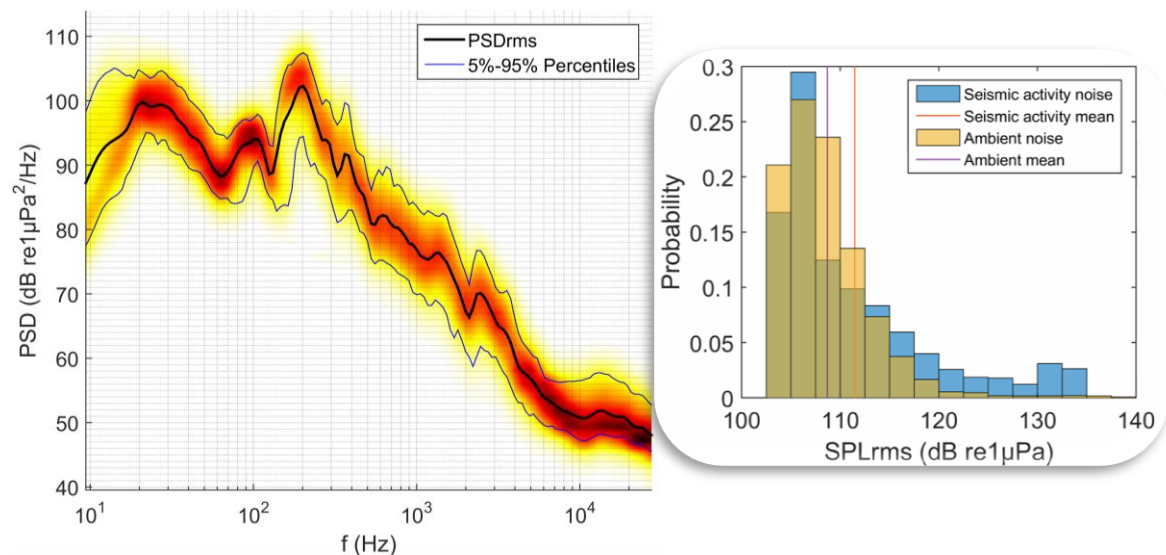


Fig. 4.4. Aggregated 30 sec PSDs concerning Zakynthos station and SPLrms histograms (din width 2.5 dBre1 $\mu$ Pa) with average value indications regarding seismic activity versus ambient noise monitoring.

### 4.3. Katakolo Station

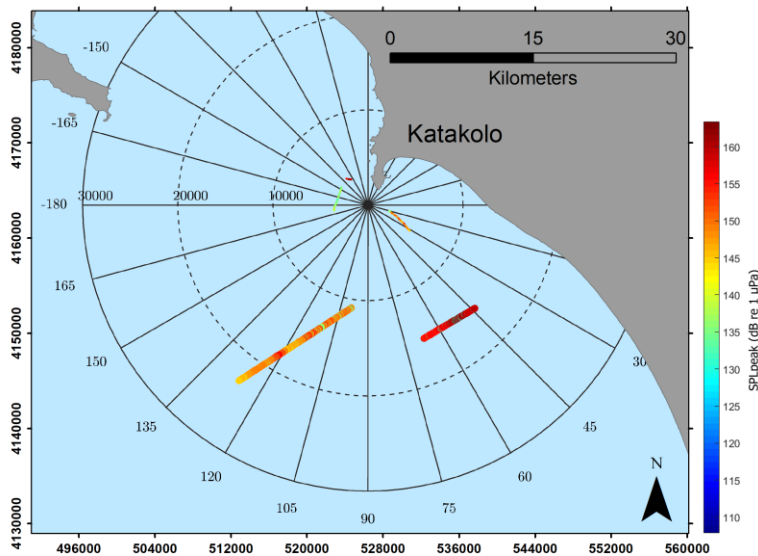


Fig. 4.5. Spatial representation of the SPLpeak of the detected seismic pulses in Katakolo station, with regard to the position of the SW COOK while executing seismic lines.

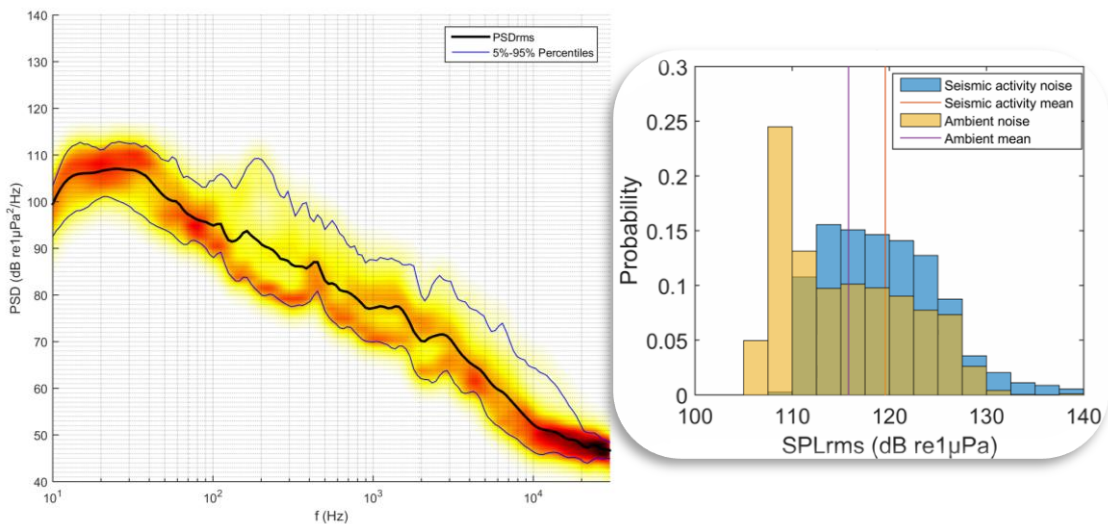


Fig. 4.6. Aggregated 30 sec PSDs concerning Katakolo station and SPLrms histograms (bin width 2.5 dB re 1 μPa) with average value indications regarding seismic activity versus ambient noise monitoring.

#### 4.4. Marathopoli Station

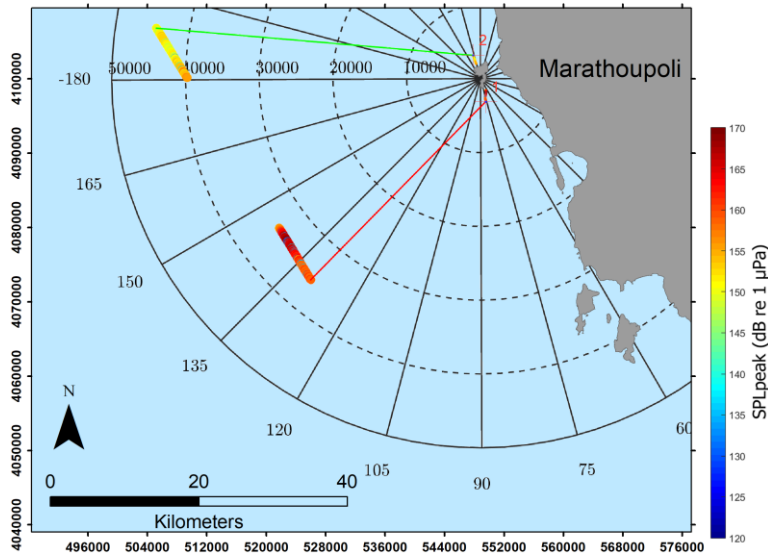


Fig. 4.7. Spatial representation of the SPLpeak of the detected seismic pulses in Marathopoli station, with regard to the position of the SW COOK while executing seismic lines.

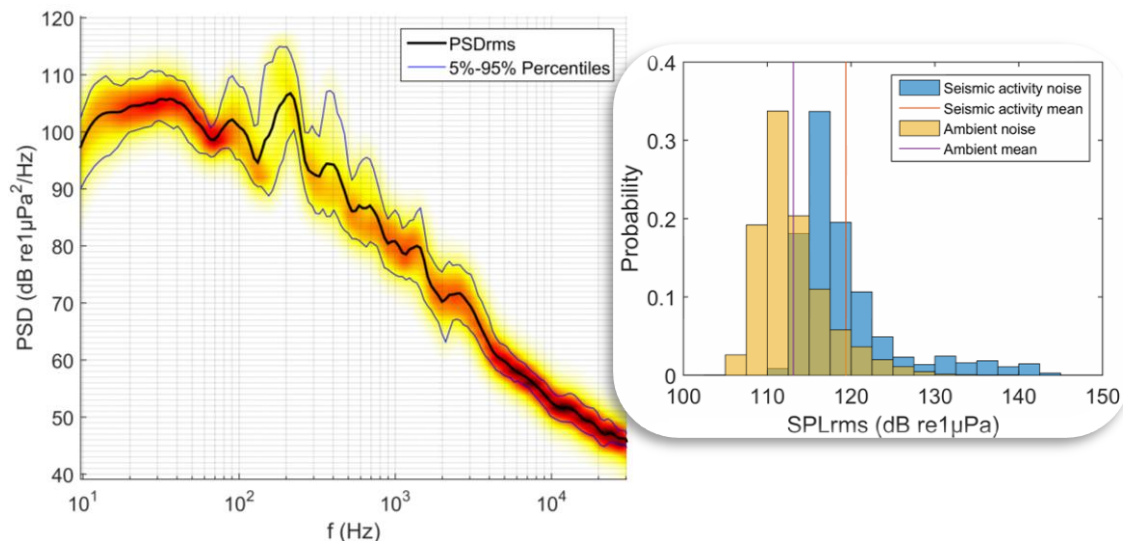


Fig. 4.8. Aggregated 30 sec PSDs concerning Marathopoli station and SPLrms histograms (bin width 2.5 dBre1μPa) with average value indications regarding seismic activity versus ambient noise monitoring .

### 4.5. Methoni Station

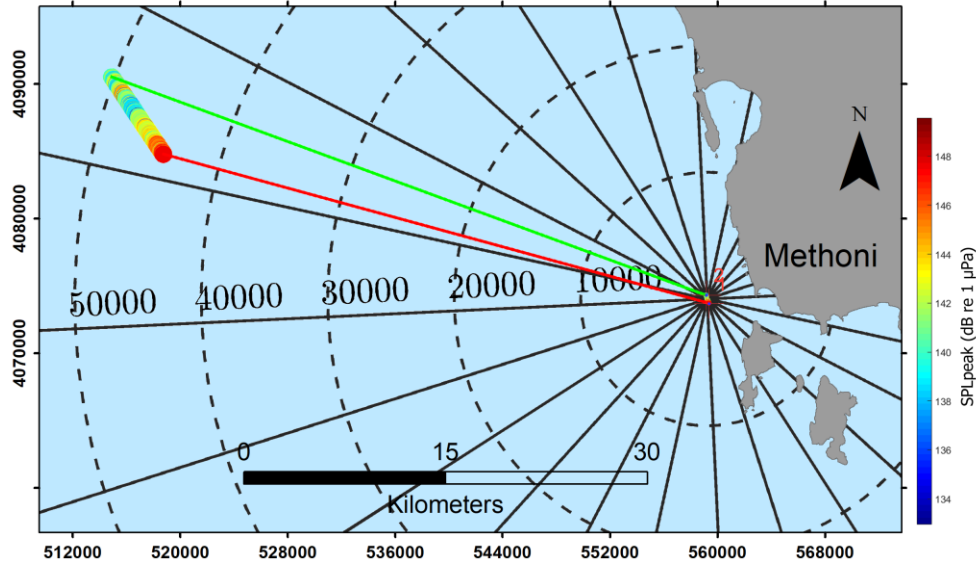


Fig. 4.9. Spatial representation of the SPLpeak of the detected seismic pulses in Methoni station, with regard to the position of the SW COOK, executing seismic lines.

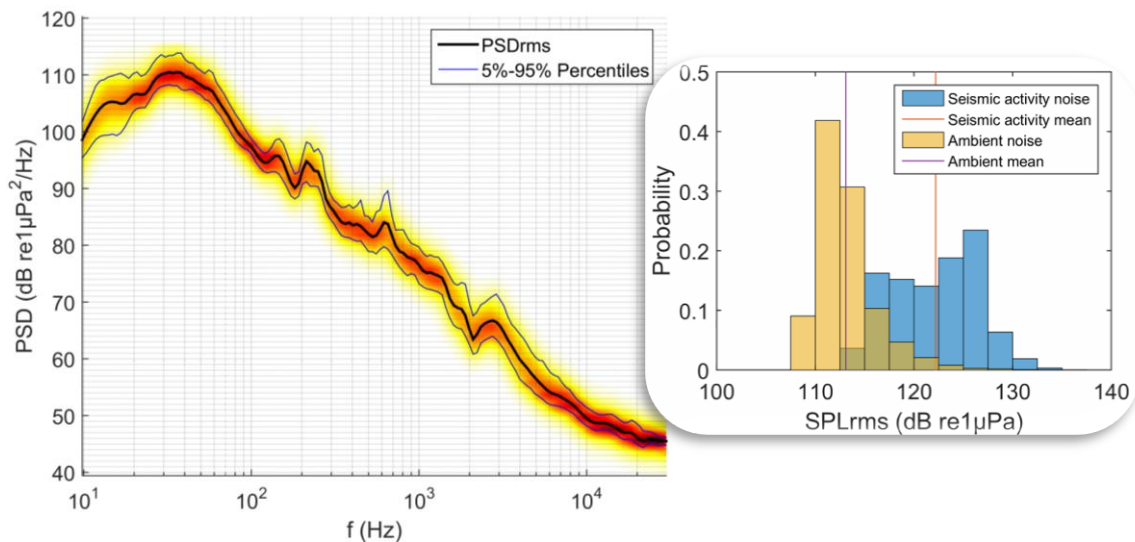


Fig. 4.10. Aggregated 30 sec PSDs concerning Methoni station and SPLrms histograms (bin width 2.5 dB re 1 μPa) with average value indications regarding seismic activity versus ambient noise monitoring.

#### 4.6. Seismic noise VS distance to the source

SPL<sub>p-p</sub> received levels of the detected seismic pulses versus the distance between SW COOK and the sound recording are given either in logarithmic (Figure 4.11) or linear (Figure 4.12) distance axis format. The data acquired during the exclusion zone verification were included in the diagrams to input estimations for the close ranges to the seismic source. A logarithmic fit has been applied to the data while its upper 90% confidence interval has been drawn to exploit the trend of the maximum received levels over distance. The maximum seismic noise presents a sharp decrease from 210 dB to 180 dB before 5km distance from the source while it gradually decreases to 165 dB 50km away.

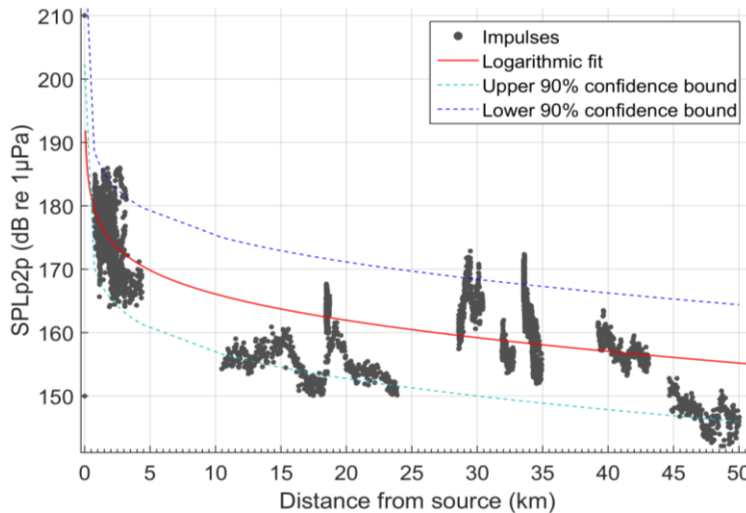


Fig. 4.11.  
The peak-to-peak SPL (SPL<sub>p-p</sub>) of each detected airgun impulses versus the linear distance to the seismic source, recorded during the seismic monitoring and exclusion zone verification phases of the project, superimposed by a logarithmic fit and its upper and lower 90% confidence intervals.

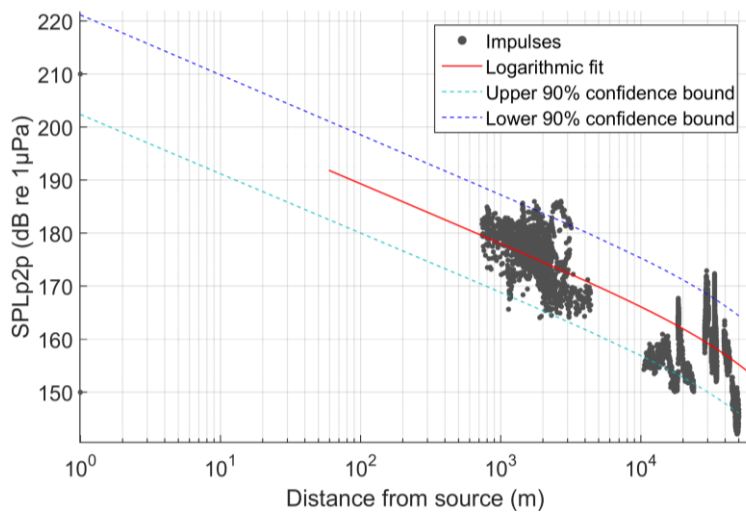


Fig. 4.12.  
The peak-to-peak SPL (SPL<sub>p-p</sub>) of each detected airgun impulses versus the logarithmic distance to the seismic source, recorded during the seismic monitoring and exclusion zone verification phases of the project, superimposed by a logarithmic fit and its upper and lower 90% confidence intervals.



## 5. Personnel

The following personnel was employed for the fieldwork and data processing stages from the Oceanus Lab, Department of Geology, University of Patras.

<b>Name</b>	<b>Responsibility</b>
<b>Prof. George Papatheodorou</b>	Project leader
<b>Dr. Dimitris Christodoulou</b>	Fieldwork leader, Data processing and reporting Personnel
<b>Dr. Elias Fakiris</b>	Data processing and reporting leader- Fieldwork Technical Personnel
<b>Dr. Nikos Georgiou</b>	Fieldwork Technical/ Data processing and reporting Personnel
<b>Mr. Alexandros Menegatos</b>	Field work Technical Personnel
<b>Capt. Gerasimos Sotiropoulos</b>	Vessel Captain

